The May/June 2008 Saharan dust event over Munich: Intensive aerosol parameters from lidar measurements

M. Wiegner,[1] S. Groß,[1] V. Freudenthaler,[1] F. Schnell,[1] and J. Gasteiger[1]

Received 27 July 2011; revised 6 October 2011; accepted 7 October 2011; published 15 December 2011.

[1] At the end of May 2008 one of the strongest Saharan dust outbreaks ever reached Central Europe. This event gave us the opportunity to extend our series of studies on Saharan dust characterization, which includes measurements near the source (SAMUM-1, Morocco) and in the regime of mid range transport (SAMUM-2, Cape Verde). The optical properties of the aerosol particles as a function of time and height are derived from data of the two Raman depolarization-lidar systems MULIS and POLIS at Munich and Maisach (Germany), respectively. Measurements include the extensive properties of the particles, backscatter coefficient β_p and extinction coefficient α_p, and the intensive particle properties, linear depolarization ratio δ_p and lidar ratio S_p. All quantities are derived at two wavelengths, $\lambda = 355$ nm and $\lambda = 532$ nm. The focus of the study is on the intensive properties, for which we found on average $\delta_p = 0.30$ at 355 nm and $\delta_p = 0.34$ at 532 nm. The systematic errors were typically larger than the δ_p-difference at the two wavelengths. With respect to the lidar ratio, we found $S_p = 59$ sr for both wavelengths, with an uncertainty range between ±4 sr and ±10 sr. These values are quite similar to the results from the SAMUM campaigns. Thus, our results suggest that the intensive optical properties of Saharan dust do not change significantly if the transport time is less than one week. However, more case studies in the far-range regime are required to scrutinize this statement. To further refine conclusions with respect to the wavelength dependence of δ_p a further reduction of the errors is desired.

Citation: Wiegner, M., S. Groß, V. Freudenthaler, F. Schnell, and J. Gasteiger (2011), The May/June 2008 Saharan dust event over Munich: Intensive aerosol parameters from lidar measurements, *J. Geophys. Res.*, *116*, D23213, doi:10.1029/2011JD016619.

1. Introduction

[2] Mineral dust is one of the major aerosol components of the atmosphere and is known to considerably influence the Earth's radiative budget [*Tegen et al.*, 1996]. Its impact strongly depends on the spatial distribution and optical properties of the aerosols [*Sokolik et al.*, 2001]. Whereas the main source regions of mineral dust are limited to the large deserts in Africa and Asia – with the Saharan desert as the most important – its impact is global and dust emission are estimated to be up to 3000 Tg per year [*Penner et al.*, 2001; *Zender et al.*, 2004; *Cakmur et al.*, 2006]. It has been shown that dust particles, lifted to the free troposphere by strong convection, can be transported over long distances: the most relevant transport path certainly is westward across the Northern Atlantic Ocean in the well-know Saharan dust layer as was already shown more than 40 years ago from surface and airborne in-situ measurements [e.g., *Delany et al.*, 1967; *Prospero and Carlson*, 1972], or more recently [*Morris et al.*, 2006]. Moreover, Saharan aerosol layers often are observed in Europe with a more complex structure; many studies [*Ansmann et al.*, 2003; *Mattis et al.*, 2002; *Mona et al.*, 2006; *Papayannis et al.*, 2008; *Guerrero-Rascado et al.*, 2009; *Córdoba-Jabonero et al.*, 2011] were performed in the framework of the European Aerosol Research Lidar Network (EARLINET) [*Bösenberg et al.*, 2003]. The purpose of these lidar studies was twofold: the observation of the vertical distribution of the aerosols and the assessment of their optical properties. Whereas the benefit of the knowledge of optical properties is obvious, the relevance of the spatial distribution for e.g. satellite-based retrievals of aerosol optical depth was demonstrated by an intercomparison of nine different algorithms [*Myhre et al.*, 2005]. They showed that in the presence of strong lofted dust layers the retrieved aerosol optical depth varies by a factor of up to three.

[3] To improve the knowledge on microphysical and optical properties of mineral dust, dedicated observations were made during several field campaigns, e.g., SHADE and ACE-Asia at the beginning of this century. Recently, two experiments took place in the framework of the "Saharan mineral dust experiment", SAMUM: the focus of the first campaign in Morocco in May and June 2006 was on pure, fresh Saharan dust [*Heintzenberg*, 2009], the second campaign was conducted at the Cape Verde Islands in January and February 2008 and dealt with mid-range transported dust and dust in different mixing states [*Groß et al.*, 2011a]. Both experiments provided excellent data sets for a full description of dust aerosols, however, characterization of dust transported in the long range regime are still rare.

[1]Meteorological Institute, Ludwig-Maximilians-Universität, Munich, Germany.

0148-0227/11/2011JD016619

[4] In this work we take advantage of one of the strongest Saharan dust outbreaks ever observed over Central Europe to investigate how dust properties change within a few days. The dust event could be observed over southern Germany in the area of Munich and lasted for more than one week starting by the end of May 2008. Our studies are primarily based on lidar measurements from the EARLINET-sites Munich (48.148°N, 11.573°E, altitude: 539 m) and Maisach (48.209°N, 11.258°E, altitude: 516 m), because they allow one to clearly separate properties of the boundary layer aerosols and the lofted dust layer. These data sets are complemented by co-located Sun photometer measurements.

[5] We concentrate on investigations of two intensive properties of dust to be compared with results from SAMUM-1 and SAMUM-2: the first is the particle lidar ratio S_p that is defined as the ratio of the extinction coefficient α_p and the backscatter coefficient β_p of the particles, the second is the particle linear depolarization ratio δ_p. Both quantities can be used to discriminate aerosol types [e.g., *Groß et al.*, 2011b]. They are useful to investigate dynamics, air quality, and to support satellite remote sensing and climate modeling. An excellent demonstration of the benefit of δ_p was recently provided in the course of the Eyjafjallajökull eruption in April 2010 [*Wiegner et al.*, 2011]. Furthermore, the assessment of the lidar ratio is of fundamental interest for the evaluation of the spaceborne lidar mission CALIPSO (Cloud-Aerosol Lidar and Infrared Pathfinder Satellite Observations [e.g., *Winker et al.*, 2007]). This mission applies a backscatter lidar, that means, the accuracy of the derived extinction coefficient profiles strongly depends on the assumed range dependent lidar ratio and its uncertainty.

[6] The paper is organized as follows: in the subsequent section we give a brief overview of the instruments involved in our study and the available data sets. Then, we review the temporal evolution of the dust event of May 2008. In section 4 we describe the derivation of two intensive optical properties (S_p and δ_p) of mid-range transported dust over Munich. Their relation to corresponding measurements closer to the dust source as performed during SAMUM is discussed in section 5. A brief summary concludes the paper.

2. Measurements and Instrumentation

[7] Range-resolved measurements presented in this work were performed with the two lidar systems MULIS (multi-wavelength lidar system) [*Freudenthaler et al.*, 2009] and POLIS (portable lidar system) [*Groß et al.*, 2008] developed and operated by the Meteorological Institute of the Ludwig-Maximilians-Universität (LMU), Munich, Germany. Both systems are reference lidars of EARLINET, that means, they have undergone strict quality assurance.

[8] MULIS is a Raman and depolarization lidar with channels for elastic backscattering at 355 nm, 532 nm, and 1064 nm, and two channels for inelastic N_2-Raman scattering at 387 nm and 607 nm. The linear depolarization ratio of particles δ_p is derived from two channels at 532 nm, separating co- and cross polarization. POLIS is a small, low power, two channel lidar, that can be operated in two configurations: either the channels are sensitive at 355 nm (elastic scattering) and 387 nm (Raman scattering), or both channels are sensitive at 355 nm, but with two perpendicular planes of polarization. We refer to these configurations as "Raman mode" and "depolarization mode", respectively. The range resolution of the raw data is 7.5 m. The optical design of both lidars allows one to retrieve aerosol profiles quite close to the ground: MULIS provides full overlap above 200 m to 500 m depending on field stop adjustments and amplifier settings, POLIS above 100 m. Furthermore, we want to emphasize that combining the measurements of both lidars provides depolarization ratios at two wavelengths. These features make MULIS and POLIS a unique set of lidar systems.

[9] Note, that δ_p can be determined at day- and nighttime. In contrast, measurements at 387 nm and 607 nm (henceforward referred to as "Raman measurements") for the determination of the lidar ratio are restricted to nighttime operation because of the high solar background during daytime. The advantage of Raman measurements is that the extinction coefficient α_p and the backscatter coefficient β_p can be determined independently, and that – as a consequence – the lidar ratio S_p can be derived [*Ansmann et al.*, 1992]. In case of daytime measurements and in case of POLIS measurements in the depolarization mode at night, we have to rely on the Klett/Fernald algorithm [*Klett*, 1985; *Fernald*, 1982] that requires S_p as an input parameter. To estimate an adequate S_p we take values from Raman measurements from the previous or following night, whichever is closer in time.

[10] As second input parameter of the Klett/Fernald algorithm a boundary value of β_p at a reference height z_{ref} is required. For this purpose an aerosol-free part of the atmosphere (typically in the upper free troposphere or in the stratosphere) is usually selected and $\beta_p(z_{\mathrm{ref}})$ is set to zero. For many of our measurements during this event this assumption could not be applied as aerosols were present throughout the troposphere up to cloud levels. As a consequence, we estimate a boundary value using the volume linear depolarization ratio δ_v as an indicator for the amount of aerosols at the reference range. This parameter can readily be determined from the ratio of the cross-polarized ($P_\perp$) and co-polarized signal ($P_\parallel$) as an accurate calibration factor C_δ of the relative sensitivity of the two channels has been provided [*Freudenthaler et al.*, 2009]. From δ_v, a boundary value $\beta_p(z_{\mathrm{ref}})$ can be determined as briefly outlined in the following.

[11] We define ϵ as the relative contribution of particles to the total backscatter coefficient, i.e.

$$\epsilon = \frac{\beta_p}{\beta} \tag{1}$$

[12] From calibrated lidar measurements the volume linear depolarization ratio δ_v can be determined via

$$\delta_v = C_\delta \frac{P_\perp}{P_\parallel} \tag{2}$$

[13] Furthermore, we use the molecular linear depolarization ratio δ_m and the particle linear depolarization ratio δ_p, defined as

$$\delta_m = \frac{d_m}{2 - d_m} \quad \text{and} \quad \delta_p = \frac{d_p}{2 - d_p} \tag{3}$$

with d_m and d_p being the depolarization parameter for molecules and aerosols, respectively. These parameters can be

Table 1. Overview Over the Lidar Measurements[a]

	MULIS		POLIS		
Date	Site	Depol. and Raman	Site	Depol. Mode	Raman Mode
23 May	MS		MU	1350–1525	
27 May	MS	1200–1500 + 2000–2400	MU	0845–2350	
28 May	MS	0000–2000 + 2230–2400	MU	0010–2210	2225–2400
29 May	MS	0000–2400	MU	0010–1910	1945–2045
30 May	MS	1100–1400 + 2030–2400	MU	1020–1340	
31 May	MS	1315–1545 + 2220–2400	MS	1310–1505 + 2000–2400	
1 June	MS	0000–0140 + 1400–2150	MS	0000–0140 + 1410–2400	
2 June	MS	0000–2130	MS	0000–2210	

[a]Times in UTC; Depol., Depolarization; site: MU, Munich; MS, Maisach.

calculated from the (1,1)- and (2,2)-element of the Mueller matrix [*Gimmestad*, 2008]. Then, ϵ can be expressed as

$$\epsilon = \frac{(1+\delta_p)(\delta_m - \delta_v)}{(1+\delta_v)(\delta_m - \delta_p)} \tag{4}$$

[14] In equation (4), δ_m is known from scattering theory and δ_v from measurements. The ratio ϵ can be calculated with a prescribed δ_p according to the aerosol type; the accuracy is best when δ_p is large. Consequently, we apply this method in cases when we are confident that the aerosol type is dust and assume $\delta_p = 0.30$ according to previous measurements. Finally, β_p is determined according to

$$\beta_p = \beta_m \left(\frac{\epsilon}{1-\epsilon}\right) \tag{5}$$

[15] The backscatter coefficient of the air molecules β_m is calculated from air density profiles derived from radiosonde ascents by means of the ideal gas law and Rayleigh theory. Applying this approach, a boundary value $\beta_p(z_{\mathrm{ref}})$ can be estimated from a measurement of δ_v. Typically we select a height range where the range corrected lidar signal suggests that the aerosol backscatter is low, and – as stated above – these aerosols are dust.

[16] Observations were made at Munich and Maisach (see Table 1). The Munich site is in the center of the city, whereas Maisach is a rural site 25 km north-west of Munich. At the beginning of the dust episode, one lidar was implemented at each site to determine mesoscale variations of the aerosol distribution. Note, that as a consequence, δ_p at 355 nm and δ_p at 532 nm were not measured at the same location. On 31 May, POLIS was transported to Maisach to have linear depolarization ratios at two wavelength strictly co-located and coincident.

[17] In addition to the lidar measurements, the Sun- and sky-photometer (Cimel CE318) of our AERONET-station in Munich provided measurements of direct spectral radiances at several wavelengths between 340 nm and 1020 nm, and scattered radiances from the almucantar geometry. These data were used to have a continuous daytime record of the aerosol optical depth (τ_p, AOD) and of derived quantities such as the frequently used Ångström exponent κ of the optical depth.

$$\kappa = \frac{\ln \tau_p(\lambda_1) - \ln \tau_p(\lambda_2)}{\ln \lambda_2 - \ln \lambda_1} \tag{6}$$

[18] Furthermore, the photometer data provide independent information for consistency checks of the lidar retrievals.

[19] In contrast to the Sun photometer measurements, MULIS- and POLIS-operation cannot be unattended. Hence, no continuous time series of lidar data is available, but we succeeded to cover all relevant time periods of the dust event. Time is given in UTC, height as "height above ground level" throughout this paper.

3. The Dust Event

[20] A very strong dust event, i.e. air masses with significant dust load from the Saharan desert, was forecast to cover Europe in May 2008. According to the dust regional atmospheric model (DREAM) [*Nickovic et al.*, 2001], the event should last from 26 May to 5 June, and peak optical depths of $\tau_p > 0.8$ (at 550 nm) should be observable in southern Germany. Thus, a very good opportunity for dust characterization by lidar measurements could be expected. To get a first overview of the atmospheric situation during this period we use passive remote sensing and backward trajectories. The detailed analysis is left to the lidar data evaluation (Section 4).

[21] Sun photometer measurements at Munich, performed in the framework of AERONET [*Holben et al.*, 1998], in general confirm the forecasts. Figure 1 shows the aerosol optical depths τ_p for λ = 1020 nm (red crosses), for λ = 532 nm (green crosses), and for λ = 380 nm (blue crosses) from Level 2.0 data (but Level 1.5 for 26 May, and Level 1.0 for 28 May) in the upper panel. The optical depth is averaged over 2.4 hours each, if more than one measurement is available during this period. The lower panel shows the Ångström exponent κ, calculated for the spectral interval from 380 nm to 1020 nm according to equation (6). It should be noted that during the whole period the cloud cover was relatively large as will be shown later in this paper. Hence, Sun photometer measurements were relatively sparse and problems due to incorrect cloud clearing might have happened, e.g., on 28 May, when the extinction coefficient exceeds $\alpha_p > 2$ (not shown in Figure 1). This is consistent with the fact that no level 2.0 data are available. Nevertheless, the corresponding κ is shown in Figure 1 (bottom).

[22] The dust episode is characterized by low Ångström exponent $\kappa \leq 0.5$, and aerosol optical depth of more than approximately 0.3 in the visible spectral range. According to these criteria Munich was affected by the dust event from 25 May (noon) until 30 May. Then, a front passage led to relatively clean air for the next two days with $\tau_p < 0.2$ in the visible and $\kappa > 1$, indicating smaller particles. On 2 June, Munich was again affected by dust as can be concluded from the increasing τ_p and the decreasing κ. We refer to the period

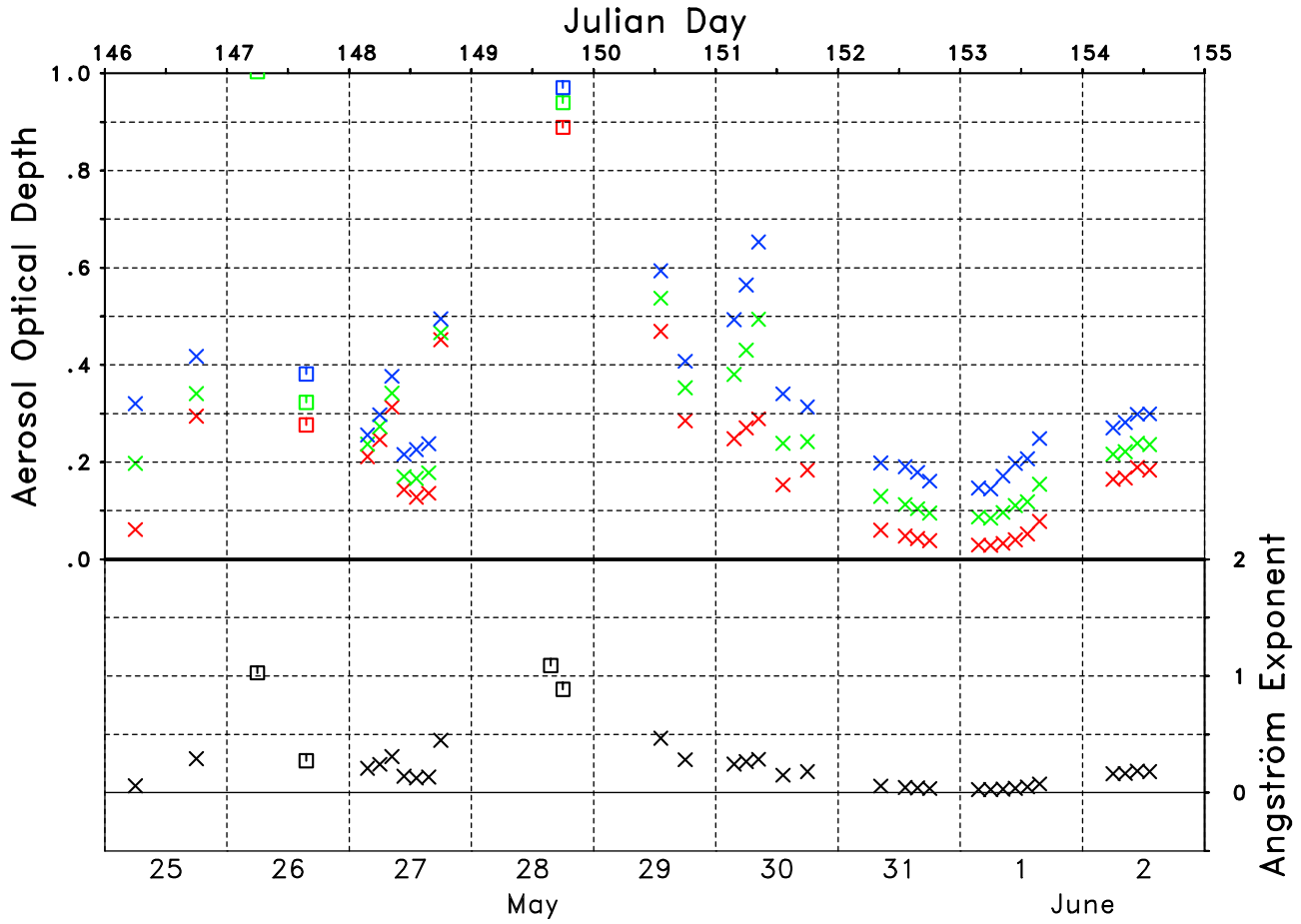

Figure 1. Aerosol optical depth (τ_p; 1020 nm, 532 nm, 380 nm in red, green and blue, respectively) and Ångström exponent (wavelength range: 380 nm/1020 nm) from the Cimel CE318 sun- and sky-photometer measurements in Munich for days as indicated. Squares denote data from Level 1.0 and Level 1.5.

before and after the front passage as the first and second phase of the dust event, respectively.

[23] The hypothesis that the aerosol over Munich was dominated by mineral dust from the Saharan desert is supported by the analysis of the synoptic situation and calculation of HYSPLIT [*Draxler*, 1988] backward trajectories: Figure 2 (left) is calculated for an arrival time of 28 May, 00:00 UTC and shows that the air masses observed in Munich and Maisach had been in contact to the lowermost atmosphere over the Saharan desert where they could uptake significant amounts of dust. During the first phase the dust plume traveled four to five days until it arrived at southern Germany directly from the south. In the second phase of the event (see Figure 2 (right), arrival time: 2 June, 03:00 UTC) the transport path was different: the dust loaded air masses arrived at Munich after three days from the west.

[24] As a consequence of the meteorological evolution of the dust event, the two phases are separately investigated with respect to a detailed optical characterization of the dust.

4. Assessment of Optical Properties

[25] The assessment of optical properties is based on our lidar measurements, They provide height resolved information that can be assigned to those atmospheric layers which are influenced by the dust. Our work covers extensive and intensive properties. The first group concerns the determination of the "abundance" of aerosols, expressed as extinction coefficient α_p or backscatter coefficient β_p as a function of height. α_p is the more relevant quantity, in particular with respect to the radiative effects of aerosols. However, the assessment of α_p requires Raman measurements and is thus limited to nighttime observations and stable atmospheric conditions. The latter is necessary as our measurements must be averaged over at least one hour. For daytime measurements, α_p can be determined with reduced, but acceptable accuracy as described in section 2. The determination of intensive properties of the particles includes the lidar ratio S_p and the linear depolarization ratio δ_p, both quantities being a function of wavelength. They can in general be used to distinguish dust aerosols from other types, but in our case these results are especially relevant as we want to extend our series of dust measurements already performed at Morocco [*Tesche et al.*, 2009; *Freudenthaler et al.*, 2009] and Cape Verde [*Groß et al.*, 2011a]. The backbone of our study are measurements of MULIS and POLIS, i.e., the same lidars already deployed in the SAMUM campaigns.

4.1. Phase 1 of the Dust Event

[26] An overview over the approach and the development of the Saharan dust plume is given as time-height cross

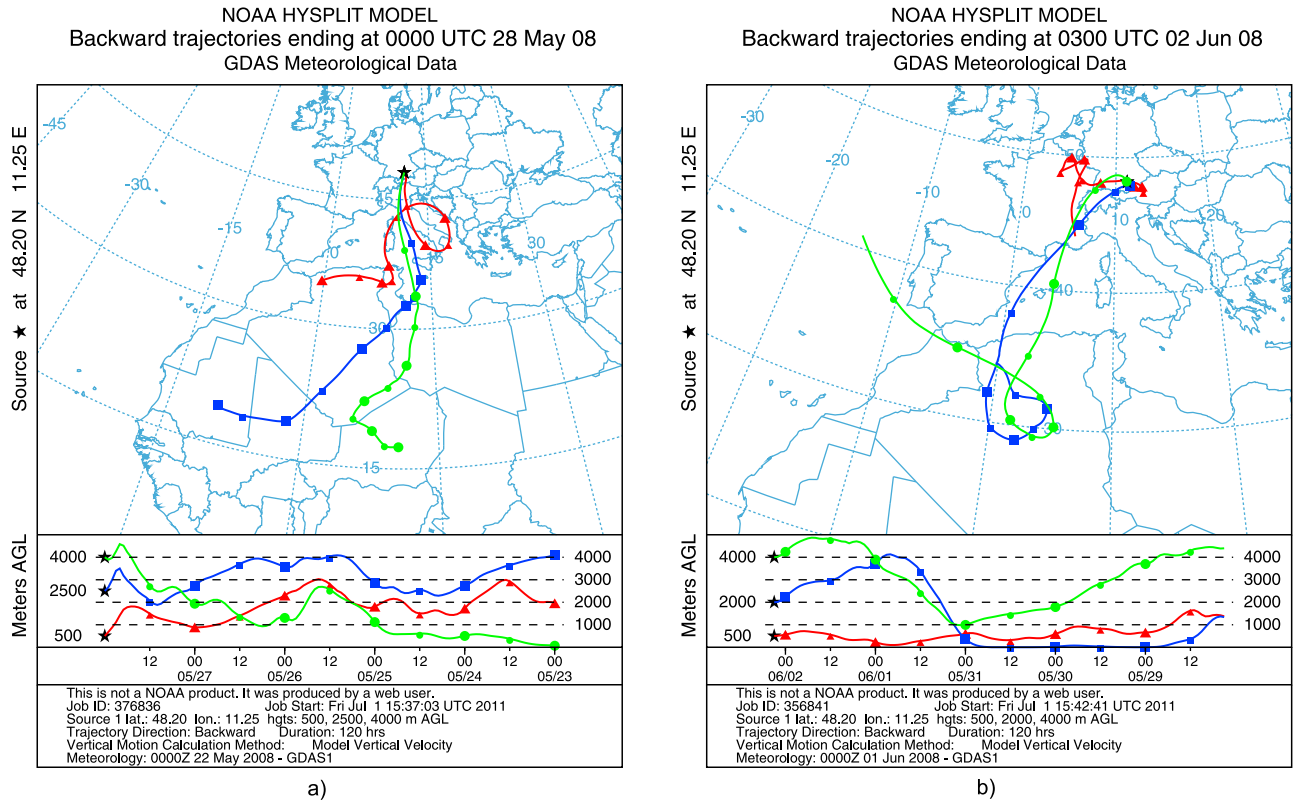

Figure 2. Calculated 5-day HYSPLIT backward trajectories of (left) 28 May 2008, 00:00 UTC and (right) 2 June 2008, 03:00 UTC for the measurement site Maisach (48.20° N and 11.25° E) for heights of 500 m, 2500 m and 4000 m above ground level.

sections ("quicklooks"). Figure 3 shows MULIS measurements over Maisach in terms of the range corrected signal at 1064 nm in logarithmic scale. The plot covers three full days from 27 May (Figure 3, top) to 29 May (Figure 3, bottom), with some breaks as indicated in Table 1. The short term disruptions of the measurements of less than one hour are due to the calibration of the depolarization channels or system adjustments. Such quicklooks are an adequate tool to select periods when the aerosol layering is stable over sufficient time to average lidar measurements for data evaluation, and to select representative time slots.

[27] Figure 3 shows that in the afternoon of 27 May (14:00 UTC) an aerosol layer above 3.0 km approaches Munich and first traces of an elevated layer in 6.5 km become visible. After 20:00 UTC the vertical distribution changes with the top of the pronounced aerosol layer around 5.0 km and a less pronounced but still significant aerosol layer up to 7.0 km. Keeping in mind that under typical conditions for Munich and for this time of the year aerosols are confined to the lowermost 2.0 km [*Wiegner et al.*, 2002], this vertical distribution is indeed an exceptional event. The small scale variability of the aerosol backscatter, in particular observed at 3.5–4.0 km in the morning of 28 May indicate mixing of dust and boundary layer aerosols. This period ends around 04:00 UTC when the upper layer disappears and a sharp upper boundary of the aerosol layer builds up at about 4.0 km. This situation remains unchanged until the end of 28 May. Starting in the morning of 29 May the vertical distribution again becomes "variable" with traces of aerosols up to 7 km (14:00 UTC) and the development of a separated layer at 4.0 km after 12:00 UTC. Nevertheless, the aerosol signature remains obvious below 4 km. Of 30 May, i.e. the end of the first phase, we only have measurements around noon, when the aerosol is confined to the lowermost 4.0 km, and at late night, when the aerosol distribution is quite inhomogeneous and low level clouds build up.

[28] Note, that almost the whole period is characterized by the presence of optically thin high clouds, which is an unfavorable situation for sun photometry.

[29] As a first step we select two one-hour periods of MULIS measurements and apply the Raman inversion methodology to derive the lidar ratios S_p. From Figure 3 we choose 27 May, 21:30 to 22:30 UTC as first period, and 28 May, 22:40 to 23:40 UTC as second period (see red boxes). Based on those lidar ratios it is possible to evaluate daytime measurements by means of the Klett method as mentioned above. Unfortunately, no adequate period is found for the evening of 29 May. On the one hand, the aerosol distribution becomes quite inhomogeneous due to mixing of dust and local aerosols, on the other hand the extinction coefficients are considerably lower than before, so that a Raman inversion cannot be performed with sufficient accuracy.

[30] Vertical profiles from the first period (27 May) are shown in Figure 4 including α_p (Figure 4, left), S_p (Figure 4, middle), and δ_p (Figure 4, right). The profiles concern wavelengths 355 nm (blue lines) and 532 nm (green lines). The pink line in the center panel is the S_p-retrieval (355 nm)

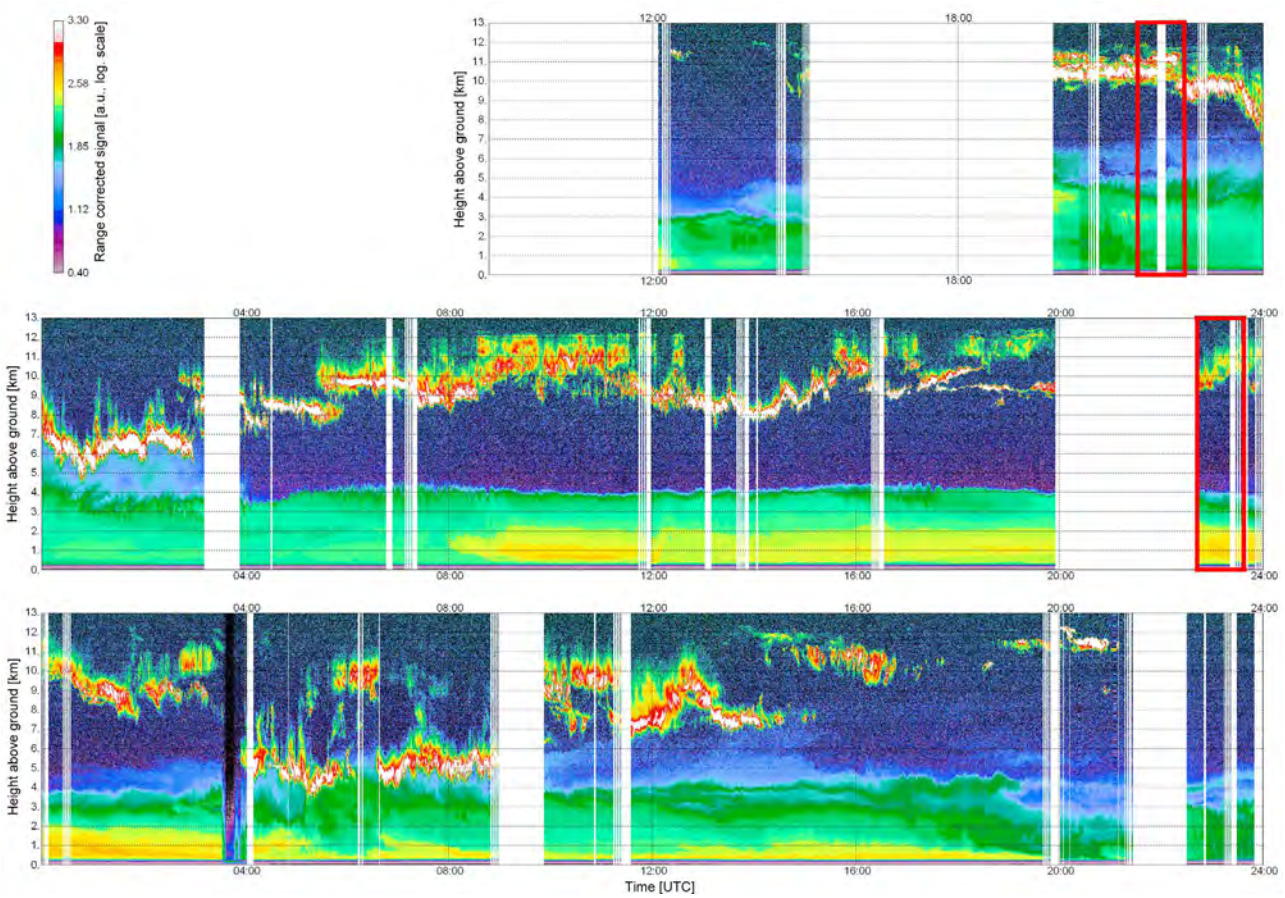

Figure 3. Development of the dust layer from (top) 27 May, (middle) 28 May and (bottom) 29 May as observed from MULIS measurements at Maisach: range corrected signal (1064 nm) in logarithmic scale, height is given in km, time in UTC. The red boxes indicate the MULIS-measurements of phases 1 and 2 shown in Figures 4 and 5, respectively.

from the corresponding 2-hour-average (27 May, 21:00 UTC to 23:00 UTC) of POLIS measurements in Munich, and shown for comparison only (see below). All other profiles are based on MULIS data in Maisach, except δ_p(355 nm) which is based on POLIS data (in Munich) from a slightly different time interval: 27 May, 19:00–20:30 UTC.

[31] The low signal-to-noise-ratios of the Raman-signals at 387 nm and 607 nm makes it necessary to smooth the signals with respect to range before optical properties can be calculated. The window length of the moving average is 652.5 m (87 range-bins) and 907.5 m (121 range-bins) at 355 nm and 532 nm, respectively. Nevertheless, the vertical structure of the aerosol distribution with two significant layers can be seen from the α_p-profiles (Figure 4, left). They show a pronounced aerosol layer extending up to 4.8 km with a maximum at 3.2 km, and a second, less pronounced aerosol layer between 5.3 km and 6.2 km. In the lower layer maximum values of $\alpha_p \approx 0.14$ km^{-1} are observed, the second layer with $\alpha_p > 0.05$ km^{-1} is weaker but still well above typical background values of 0.01 km^{-1}. To assess the optical properties of the dust, we concentrate on the height range of maximum extinction between 2.3 km and 4.3 km as indicated by the yellow area in Figure 4. The AOD of this height range is $\tau_p = 0.19$ and $\tau_p = 0.20$ at 355 nm and 532 nm, respectively, i.e., the aerosol optical depth is virtually wavelength-independent over the spectral range of the lidar wavelengths. This suggests that the particles are large as expected for mineral dust. The vertically averaged lidar ratio of this layer is $S_p = 58 \pm 8$ sr at $\lambda = 355$ nm and $S_p = 61 \pm 6$ sr at $\lambda = 532$ nm. The uncertainties given are the mean systematic errors of the lidar ratio retrieval. Taking into account the error-bars, the retrieved S_p is also wavelength-independent.

[32] The lidar ratio retrieval from POLIS measurements at 355 nm (Figure 4, pink line) results in $S_p = 57 \pm 10$ sr. This is in very good agreement with the MULIS results, though the sites are separated by 25 km and the averaging times are not identical. This is a strong indication, that the intensive aerosol properties do not change over these spatial scales, and a joint consideration of MULIS- and POLIS-results is justified.

[33] The same evaluation is done for the second period on 28 May, shortly before midnight. We select measurements of MULIS (532 nm, 22:40–23:40 UTC) and POLIS (355 nm, 22:30–24:00 UTC) to retrieve S_p. Again, the POLIS measurements to derive δ_p(355 nm) are slightly earlier (21:20–22:00 UTC). The resulting profiles are shown in Figure 5, as before, α_p, S_p, and δ_p from left to right, and the layer that is used to determine the intensive properties of dust (1.2 km to 3.0 km) is marked yellow. The profiles reveal differences of the extensive properties to the night before: there is an obvious increase of the aerosol extinction coefficient

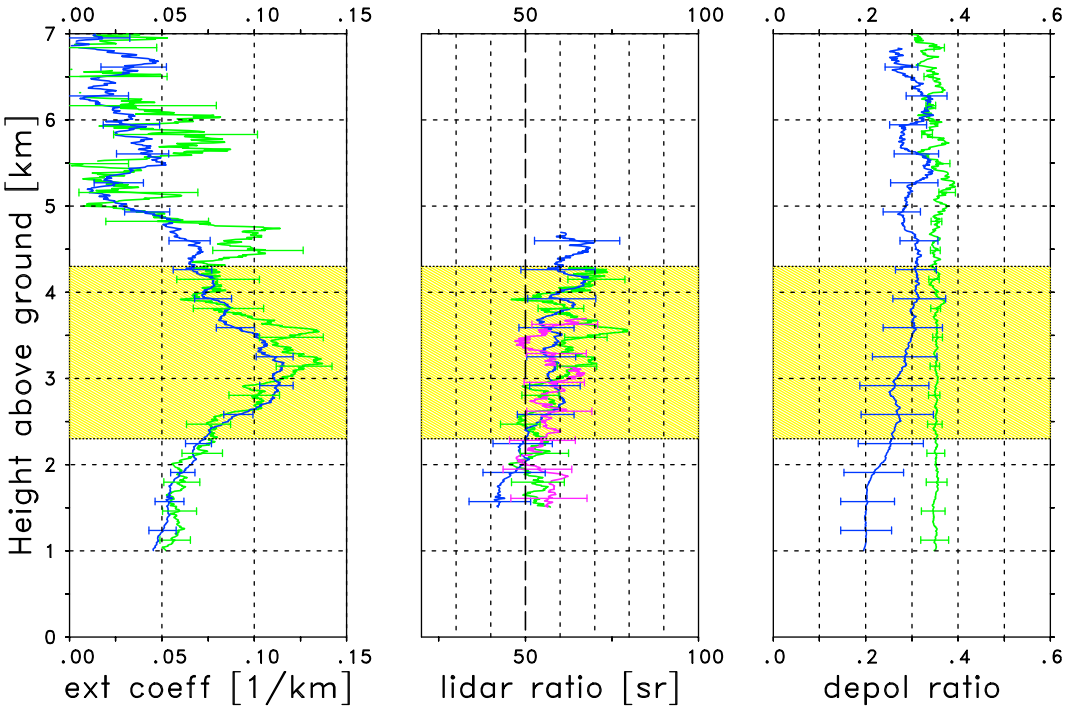

Figure 4. (left) Particle extinction coefficient α_p (in km^{-1}), (middle) lidar ratio S_p (in sr), and (right) particle linear depolarization ratio δ_p on 27 May 2008 (late evening; for details, see text). The vertical axis is height above ground (in km). Green lines correspond to 532 nm, blue lines to 355 nm. The pink line (Figure 4, middle) is for the POLIS retrieval at 355 nm. The error bars indicate the systematic errors, in case of α_p the sum of the statistical and systematic error. The measurement site is Maisach in case of MULIS (α_p, S_p and δ_p(532 nm)), and Munich in case of POLIS (S_p(355 nm), δ_p(355 nm)).

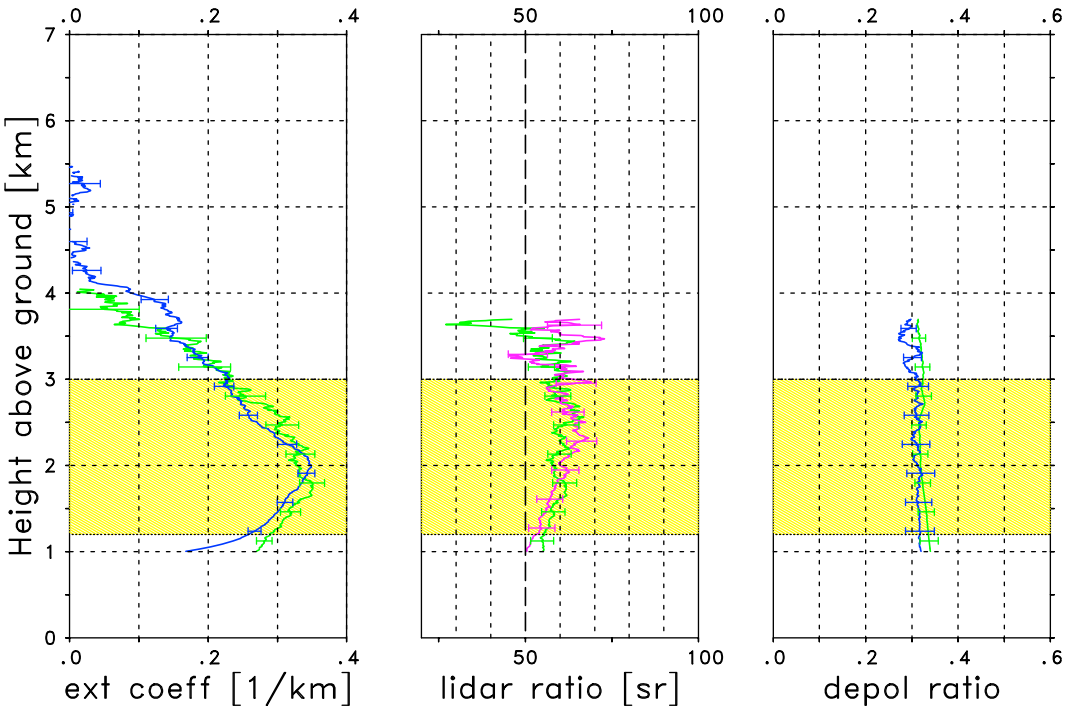

Figure 5. Same as Figure 4 but for 28 May 2008 (22:40–23:40 UTC).

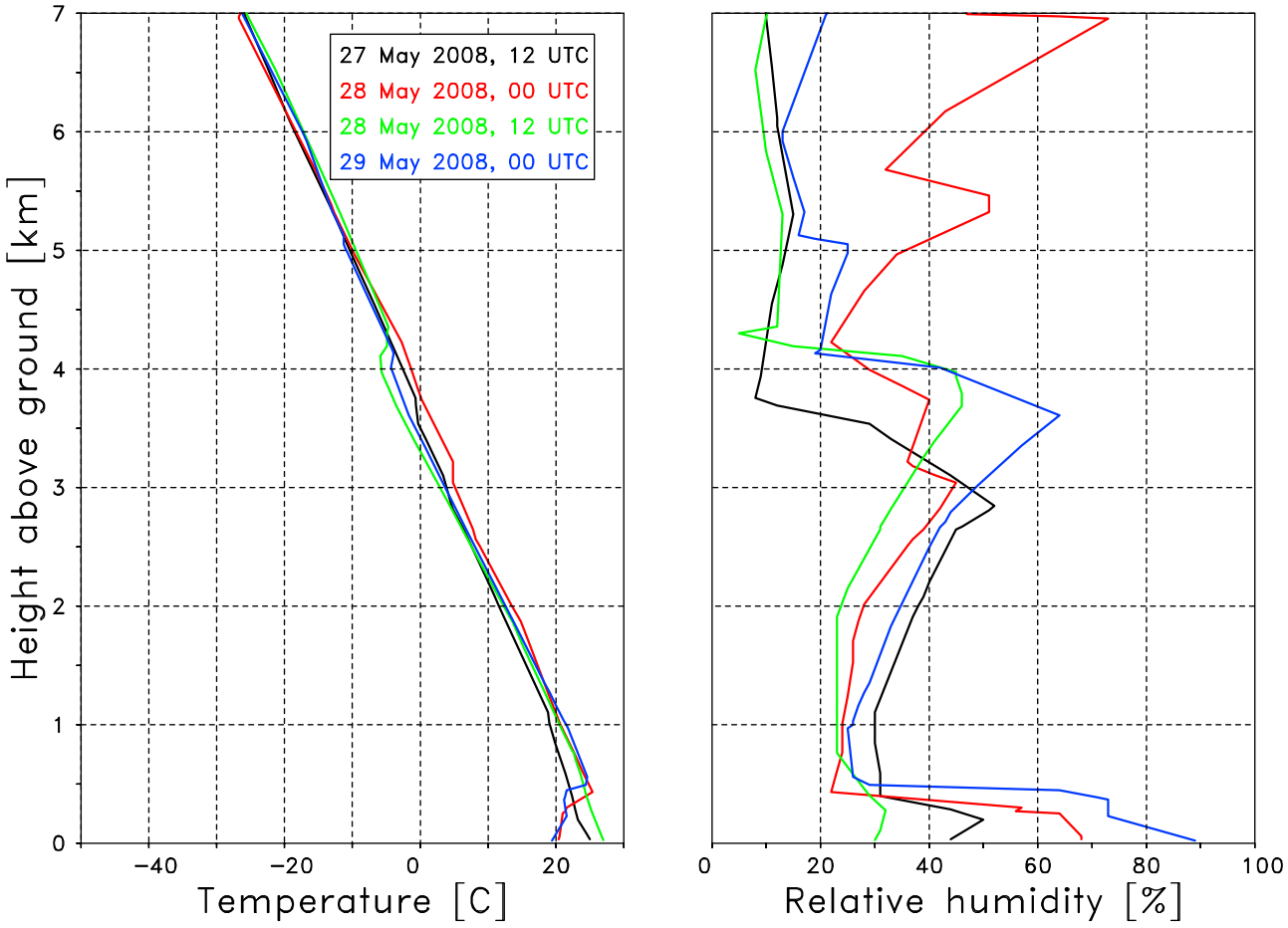

Figure 6. (left) Temperature profile (in °C) and (right) relative humidity (in %) from radiosonde ascents in Oberschleißheim: dates as indicated.

corresponding to an AOD of τ_p = 0.53 and τ_p = 0.55 at 355 nm and 532 nm, when averaged over the main layer from 1.2 km to 3.0 km. In contrast the intensive properties remain almost unchanged when compared to the previous day. The Ångström exponent based on the dust optical depth of the layer is $\kappa \approx -0.13$, and the lidar ratios at both wavelengths are found to be $S_p = 60 \pm 4$ sr.

[34] The stability of the lidar ratio suggests no changes of the microphysical properties of the aerosols. To critically analyze this hypothesis, inspection of the particle linear depolarization ratio may help. Note, that the determination of δ_p according to

$$\delta_p = (\delta_v + 1)\left(\frac{\beta_m(\delta_m - \delta_v)}{\beta_p(1 + \delta_m)} + 1\right)^{-1} - 1 \qquad (7)$$

requires the knowledge of δ_v and the β_p-profiles at the corresponding wavelengths, the latter retrieved applying the Klett inversion. As shown in Figure 4 (right) the depolarization ratio, when averaged over the highlighted height range, is $\delta_p = 0.29 \pm 0.07$ at 355 nm and $\delta_p = 0.35 \pm 0.01$ at 532 nm on 27 May. One day later, on 28 May (Figure 5, right), we find $\delta_p = 0.31 \pm 0.03$ at 355 nm and $\delta_p = 0.32 \pm 0.02$ at 532 nm. One might interpret these differences as a slight increase of the linear depolarization ratio with wavelength, but taking into account the errors, in particular at 355 nm, these changes are not significant.

[35] To get further insight we determine δ_p with a higher temporal resolution. For this purpose we use β_p as calculated from the Klett inversion, each evaluation representing an average over 30 min or 60 min in case of MULIS and POLIS measurements, respectively. The lidar ratios S_p are taken from the Raman method as shown in Figures 4 and 5. In this context it is beneficial that the S_p is only weakly height-dependent. Reasons are that obviously the layer is well mixed below a temperature inversion, and the relative humidity is mostly lower than 50% throughout the dust layer, as can be seen in Figure 6. Thus, hygroscopic growth of the particles is unlikely.

[36] Depolarization ratios based on MULIS and POLIS data, fulfilling two quality criteria, are shown in Figure 7. The criteria are: the mean (vertically averaged over the layer) retrieval error of δ_p is below 0.05, and the relative standard deviation over the vertical range is less than 1.5%. By choosing these criteria we ensure, that only stable atmospheric conditions and high quality retrievals are considered. The resulting δ_p are averaged over the common height range from 1.2 km to 2.5 km, i.e., a slightly narrower range than the highlighted range in Figure 4 because of the reduced

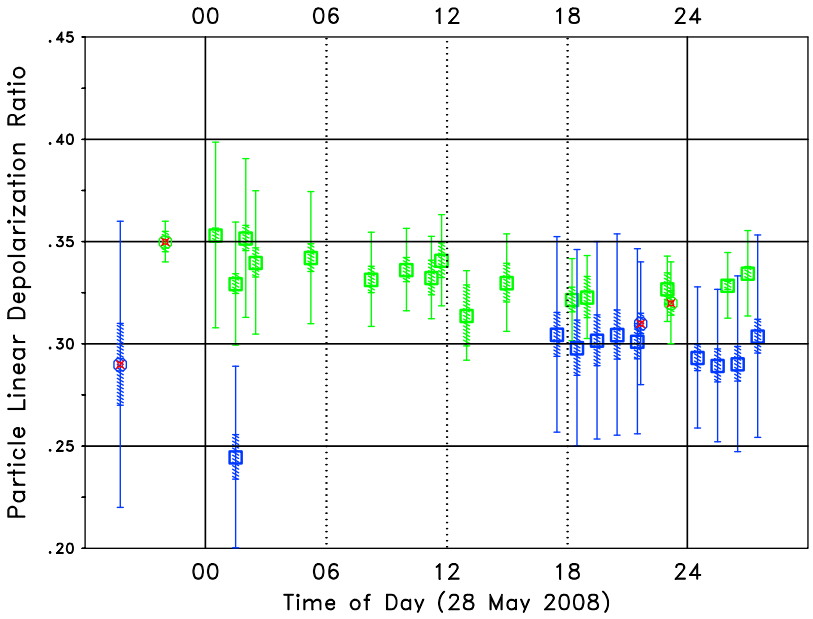

Figure 7. Particle linear depolarization ratio δ_p of the dust layer at 532 nm (green) and 355 nm (blue), average over height range as specified in the text (squares), standard deviation over height (hatched ranges), and mean retrieval error (vertical lines). Red circles indicate averages of the two periods on 27 May and 28 May shown in Figures 4 and 5. The horizontal axis is the time of 28 May (UTC).

signal-to-noise ratio during daytime. Depolarization ratios are shown as squares, blue for 355 nm and green for 532 nm. The vertical variability of δ_p is illustrated by the hatched areas and is quite small confirming that the depolarization ratio is virtually constant with height within the dust layer. The mean uncertainty of the retrieved δ_p is larger (colored error bars), in particular at 355 nm where we rely on POLIS measurements. The measurements discussed in Figures 4 and 5 (from the two periods where we performed the Raman measurements) are marked by the red crosses.

[37] Figure 7 suggests that δ_p at 355 nm is smaller than δ_p at 532 nm: the mean difference is 0.04 when averaged over all measurements displayed. One should, however, remind, that the mean uncertainty of the retrieval is slightly larger than this difference, thus, wavelength independent depolarization ratios are not in conflict with the retrievals.

[38] Finally, we want to emphasize that $\tau_p = 0.8$ at $\lambda = 532$ nm is really remarkable taking into account that typically $\tau_p < 0.2$ at Munich.

4.2. Phase 2 of the Dust Event

[39] For investigations of the second phase of the dust event we moved POLIS to Maisach to have both lidars side by side. Again, we select an adequate time period from the quicklooks of the range corrected signal at 1064 nm of MULIS, the situation until noon is shown in Figure 8. It shows an aerosol layer with distinct internal layers but a quite stable top between 5.0 km and 6.0 km.

[40] We choose the early night of 2 June for the optical characterization of the aerosols: we average MULIS data over 90 minutes from 00:00 UTC till 01:30 UTC. The profiles of α_p, S_p and α_p are shown in Figure 9 as a function of height

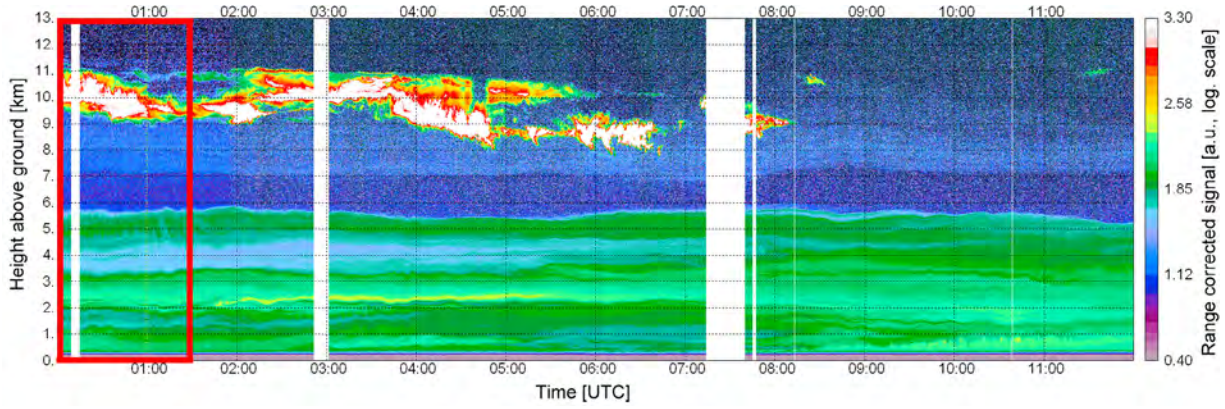

Figure 8. Time/height cross section of range corrected lidar signal of 2 June 2008 (00:00 UTC – 12:00 UTC) at Maisach as observed with MULIS (logarithmic scale, $\lambda = 1064$ nm); height is given in km. The red box indicates the time period of the retrieval shown in Figure 9.

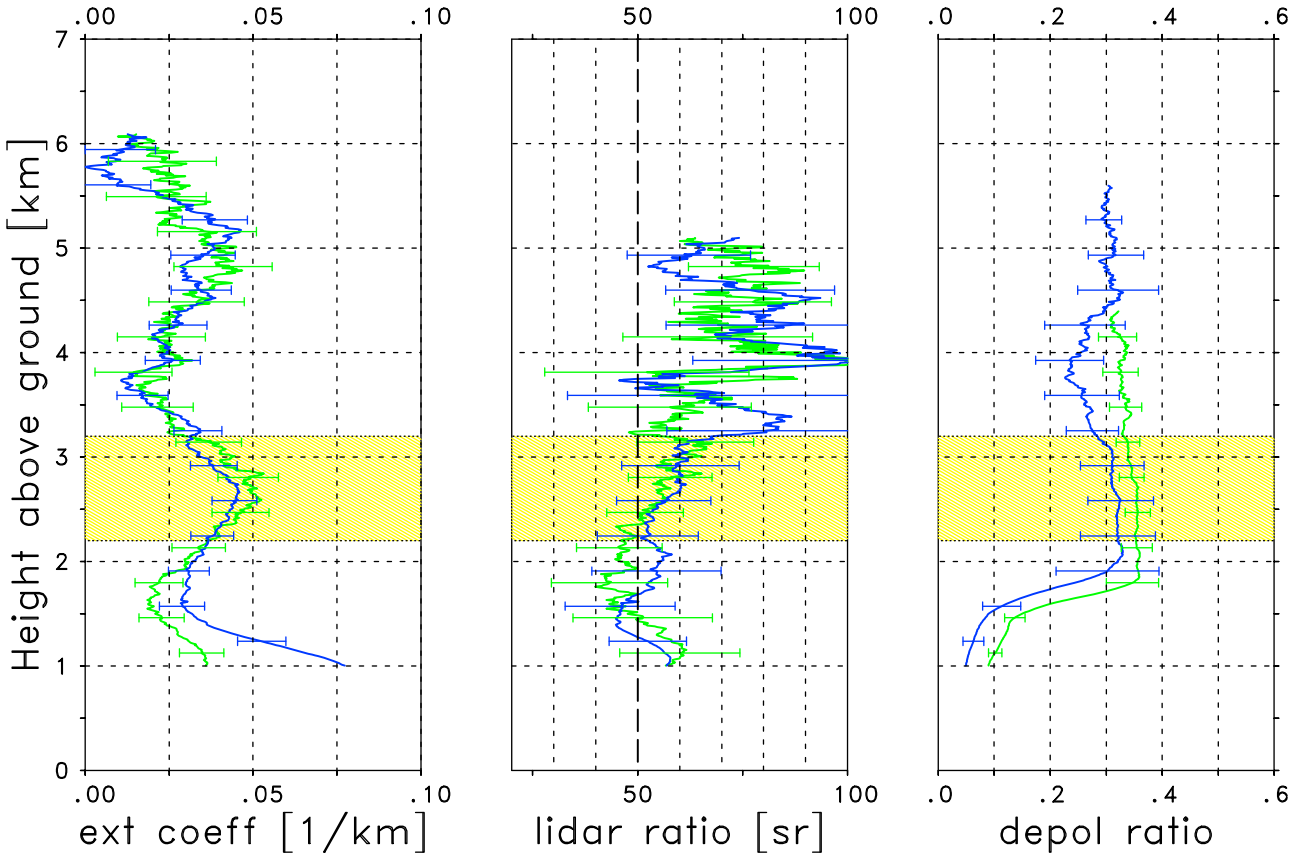

Figure 9. Same as Figure 4 but for 2 June 2008 (00:00 UTC–01:30 UTC).

above ground. POLIS is operated in the depolarization mode (see Table 1), to get depolarization ratios at two wavelengths.

[41] It can be seen that the vertical layering of the aerosol distribution is different from the first phase of the dust event. The extinction coefficient profile shows three pronounced layers, the first with its maximum below 1.3 km, the second with a maximum at 2.7 km and the third at 5.2 km. The lowermost layer certainly is not the transported dust as observed before, but a mixture of dust and locally produced aerosols. This is evident from the strong wavelength-dependence of the mean α_p ($\kappa \approx 1.6$) and the significantly lower δ_p.

[42] The extinction coefficient of the dust layers has significantly decreased compared to the first phase: α_p of the elevated layers is below 0.05 km^{-1} at both wavelengths. To make the aerosol load comparable with the first phase, we calculate again the aerosol optical depth from ground to 4 km: it is $\tau_p = 0.19$ and $\tau_p = 0.14$ at $\lambda = 355$ nm and 532 nm, respectively. The uncertainty of these numbers has already been discussed above. Nevertheless, it is clear that τ_p has decreased by a factor of approximately four. Note, that $\kappa = 0.82$ for the whole range – derived from the optical depths based on the lidar retrievals – is difficult to interpret in terms of particle properties as it combines different amounts of different types of particles. However, it compares reasonably well with the Sun photometer data ($\kappa = 0.49$; see Figure 1).

[43] The assessment of the intensive dust properties S_p and δ_p is performed as before, however, the comparably low aerosol optical depth limits the accuracy of the Raman retrievals. We select the range from 2.2–3.2 km for the assessment. The optical depth is almost the same for both wavelengths (0.039 and 0.044 at 355 nm and 532 nm, respectively), thus κ is similar to the first phase ($\kappa \approx -0.29$). This points to large particles again. From Figure 9 we find $S_p = 58 \pm 13$ sr at 355 nm, and $S_p = 56 \pm 10$ sr at 532 nm, if the systematic errors are considered. The variability with height within the highlighted range is 4 sr and 6 sr, respectively.

[44] For the investigation of the depolarization ratio we again combine the measurements of MULIS and POLIS to get the wavelength dependence. Due to the different signal-to-noise ratios of the lidar, we have to select slightly longer time periods for POLIS: here we average over 120 min from 00:55 until 02:55 UTC. The resulting δ_p are shown in Figure 9 (right). It shows a significant difference between the lowest layer and the highlighted layer: whereas for the latter $\delta_p = 0.31 \pm 0.06$ at 355 nm and $\delta_p = 0.35 \pm 0.02$ at 532 nm as expected for dust aerosols from the previous measurements, the depolarization ratio of the lower layer is $\delta_p < 0.1$, confirming, that this layer has a significant contribution of non-depolarizing, probably locally produced aerosols. The depolarization ratio of the dust layer again seems to increase with wavelength, however, the large errors at $\lambda = 355$ nm prohibit an unambiguous conclusion. Compared to the situation of phase 1, δ_p is almost unchanged. We conclude that the elevated layer around 3 km still contains the same type of

Table 2. Overview Over the Intensive Aerosol Properties δ_p and S_p at 3 Days of the Dust Event[a]

Date	Height Range	δ_p ave	δ_p err	δ_p std	δ_p max	δ_p min	S_p ave	S_p err	S_p std	S_p max	S_p min
					355 nm						
27 May	2.3–4.3	0.29	0.07	0.02	0.310	0.261	58	8	4	63.7	53.4
28 May	1.2–3.0	0.31	0.03	0.005	0.318	0.305	60	4	4	65.2	54.5
2 June	2.2–3.2	0.31	0.06	0.009	0.323	0.303	58	13	4	61.8	52.3
					532 nm						
27 May	2.3–4.3	0.35	0.01	0.005	0.356	0.348	61	6	8	69.9	50.4
28 May	1.2–3.0	0.32	0.02	0.006	0.333	0.317	60	4	2	63.4	56.8
2 June	2.2–3.2	0.35	0.02	0.007	0.356	0.339	56	10	6	63.8	47.7

[a]The time of the corresponding measurements is given in the text. Height ranges of the layers are given in kilometers and S_p in steradians; ave, average over layer; err, mean systematic retrieval error; std, vertical variability; max, 0.9-percentile; and min, 0.1-percentile.

transported dust as during the first phase, and that this dust is virtually not mixed with other particles.

4.3. Summary of the Dust Event

[45] An overview of the most relevant results of our study is given in Table 2: it comprises the intensive properties S_p and δ_p of transported dust. They are determined for the height ranges as indicated in the second column. For both quantities several parameters are listed: "ave" is the average over the layer, "err" the average of the retrieval error, "std" the standard deviation of the retrieved quantity over height describing the vertical variability, and "min" and "max" are the 10% and 90% percentile, respectively, of the retrieved quantity. Small values of the standard deviation and small differences between the 90% and the 10% percentiles indicate quantities that are practically constant with height. This is in particular the case for δ_p. Table 2 reveals that the results from the three days does not show large differences, thus, there are no indications for a temporal change during the dust event. On average we find: $\delta_p = 0.30 \pm 0.07$ at 355 nm, $\delta_p = 0.34 \pm 0.03$ at 532 nm, and $S_p = 59$ sr at both wavelengths. The uncertainty of the lidar ratio is between ±4 sr and ±10 sr in case of large and low optical depth, respectively.

[46] We want to briefly discuss two additional aspects of the lidar data: the potential for validating transport models and comparisons with independent measurements.

[47] The aerosol optical depth from the lidar measurements is one parameter that can be used to check the forecasts of the DREAM model mentioned in section 3. For this purpose, we use α_p retrievals according to the Klett-algorithm as described above. The extinction coefficient profiles are extrapolated from the first retrieval height to the ground (assuming no height-dependence) to estimate the contribution in the lidar's overlap-region. The upper boundary is set to 4.0 km for all τ_p-calculations, to avoid consideration of height ranges above the main layer, and ranges that are strongly affected by signal noise. The results for 28 May (Figure 10) show a pronounced increase of τ_p in the course

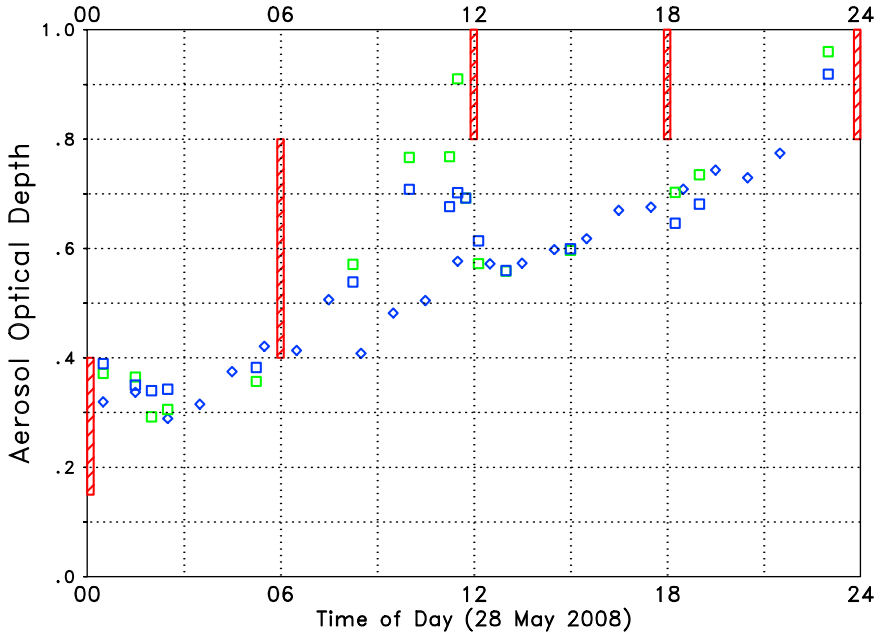

Figure 10. Aerosol optical depth from ground to 4 km derived from integrating lidar measurements of α_p: 355 nm in blue, 532 nm in green, diamonds of POLIS, squares for MULIS. The corresponding DREAM forecasts (36 hours to 60 hours) of τ_p-ranges at 550 nm are plotted in red: 0.15–0.4, 0.4–0.8 and 0.8–2.5.

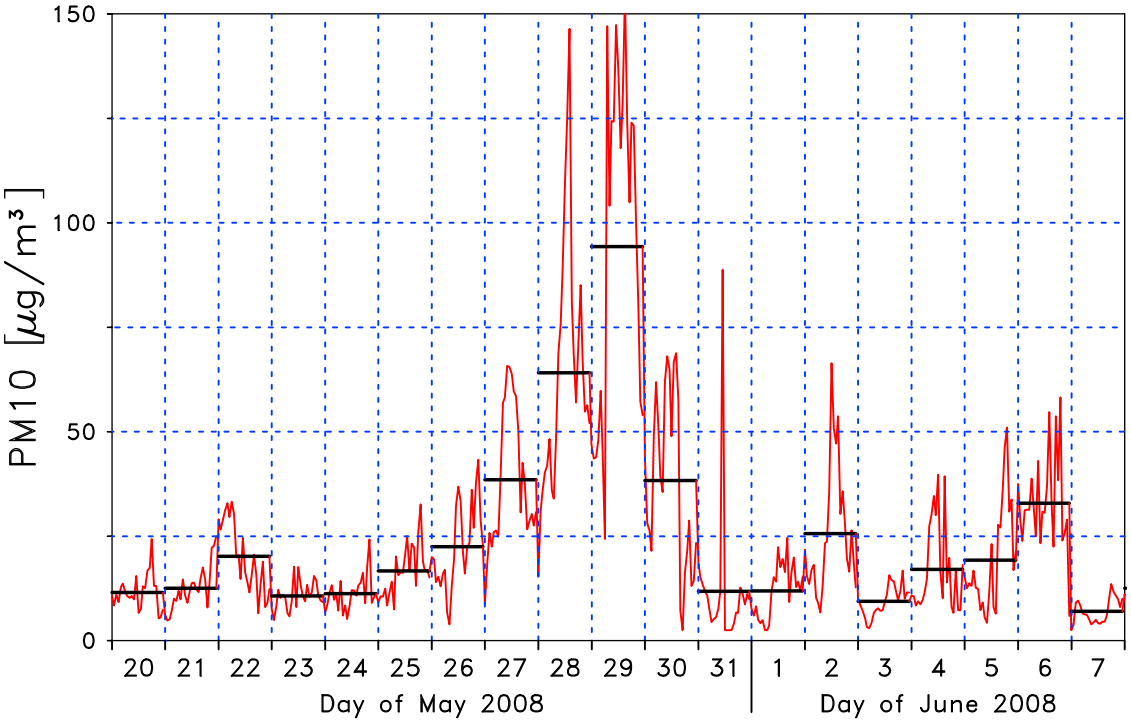

Figure 11. Time series of hourly PM10 (in $\mu g/m^3$) mass concentration at Andechs/Rothenfeld (data from the Bavarian Environmental Agency) from 20 May until 7 June 2008; the black horizontal lines denote daily averages.

of the day. The DREAM forecasts, calculated for 36 to 60 hours, provide three ranges of dust optical depth τ_p at 550 nm (0.15–0.4, 0.4–0.8, and 0.8–2.5); they are marked in red. If this quite coarse resolution is taken into account, the agreement with the lidar retrieval is acceptable with respect to the temporal development and the predicted ranges of τ_p. Note, that the lidar retrieval shown in Figure 10 rather underestimates the optical depth, as no contributions from above 4.0 km are considered. We have not added error bars to the τ_p-values, as it is not possible to elaborate a consistent error analysis, because several potential contribution are unknown. For example, we want to mention that the assumed optical depth of the "extrapolated range" (in the overlap region) is between 0.02 and 0.15. If there is a strong α_p-gradient in this height range, errors of τ_p up to the order of 0.1 might occur. Additional errors can be expected when aerosol contributions at the top of the dust layer would be missed: typically, $\alpha_p \approx 0.15$ km^{-1} in 4.0 km and decreases significantly with height, consequently, it can be expected that τ_p is not underestimated by more than approximately 0.1.

[48] Finally, we want to mention that the dust event can also be observed by ground based in-situ measurements. Higher than normal PM10 concentrations are observed in large parts of Germany [*Bruckmann et al.*, 2008]. Daily averages of the particle mass concentration (PM10) exceed 50 $\mu g/m^3$ (limit according to European regulations) in southern Germany on 28 and 29 May as determined from the monitoring network of the Bavarian Environmental Agency (H. Hanne, Bayerisches Landesamt für Umwelt, personal communication, 2010). The rural station of Andechs/Rothenfeld (35 km south-west of Munich) shows e.g. hourly mean PM10 values of up to 147 $\mu g/m^3$ for 28 and 29 May as can be seen in Figure 11. After the frontal passage the mass concentration is in general considerably lower, with only a short-time maximum of 78 $\mu g/m^3$ on 2 June. Hence, the temporal development of the event is reflected in the ground based data and in our lidar derived optical properties in a consistent way.

5. Comparison With SAMUM Results

[49] As a result of this study, we are able to extend our series of dust measurements from the source region (Ouarzazate, Morocco, SAMUM-1) [*Freudenthaler et al.*, 2009] and under conditions of mid-range transport (Cape Verde, SAMUM-2) [*Groß et al.*, 2011a] to long-range transport conditions (Munich). Thus, possible changes of the properties of dust as it ages can be studied. An overview over δ_p at 355 nm and 532 nm is given in Figure 12. For each campaign a set of depolarization ratios is given for a certain number of days (4, 8, and 3, respectively), in case of the "Munich measurements", the depolarization ratios from Table 2 are included. From our point of view the two most obvious findings are: first, the change of δ_p with age of the dust is small, and second, the absolute values are of the order of 0.30. The wavelength dependence of δ_p cannot be ultimately assessed because the uncertainty ranges due to systematic errors – in particular in case of the Munich measurements – overlap. One reason is that the laser power of POLIS has decreased after the SAMUM-2 campaign, resulting in comparably large errors of δ_p at 355 nm. Under conditions when very accurate retrievals could be achieved (primarily in the frame work of SAMUM-2), $\delta_p(355\text{ nm}) < \delta_p(532\text{ nm})$ was found, but never a decrease of the depolarization ratio with wavelength.

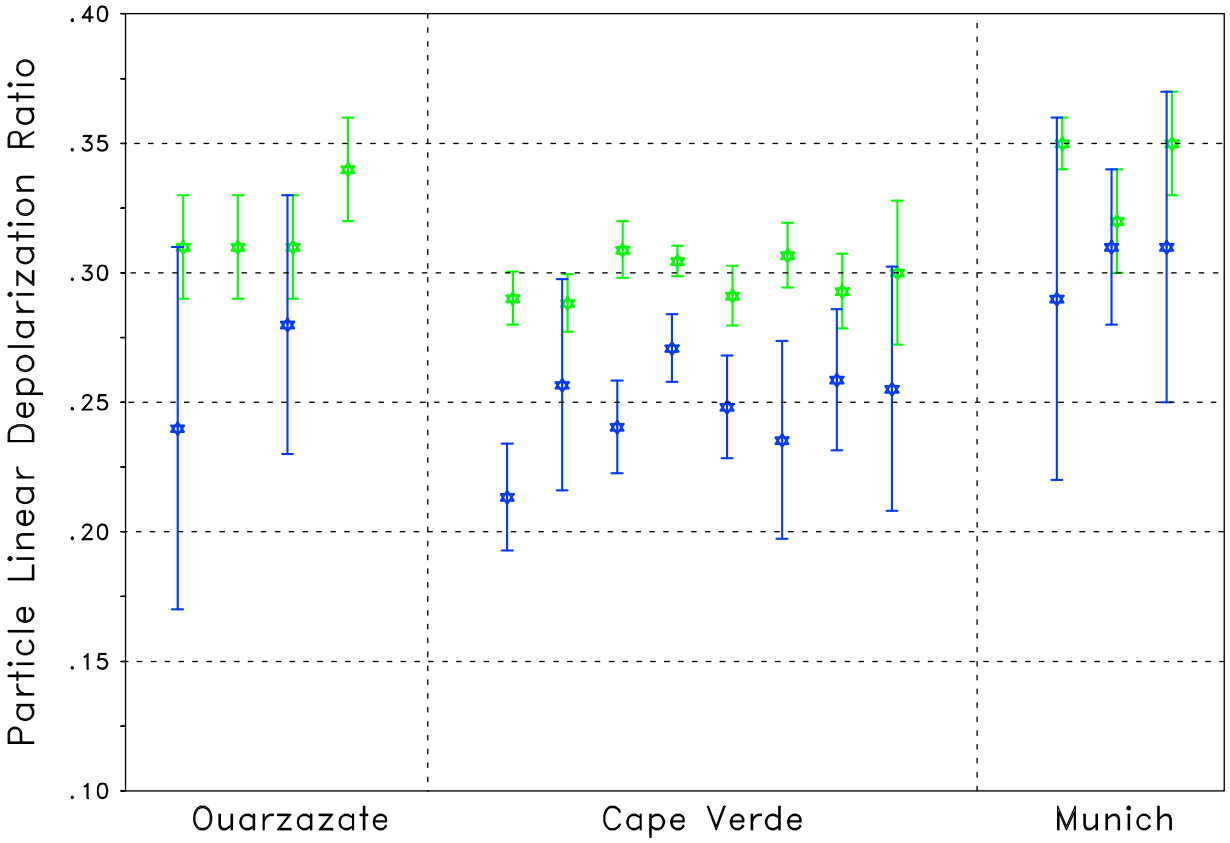

Figure 12. Particle linear depolarization ratio δ_p of Saharan dust at 355 nm (blue) and 532 nm (green) as derived on 4 days in the framework of SAMUM-1 (Ouarzazate, 2006) [*Freudenthaler et al.*, 2009], on 8 days during SAMUM-2 (Cape Verde, 2008) [*Groß et al.*, 2011b] and the 3 days of this study (Munich, 2008). Error bars denote the systematic errors.

[50] Similarly, we investigate possible changes of the lidar ratio S_p of Saharan dust from the source to the long range regime. An overview is given in Figure 13. Again, results from the present study and different days of SAMUM-2 are shown. Furthermore, we include mean values from SAMUM-1 measurements that were evaluated by *Tesche et al.* [2009] who found virtually wavelength-independent lidar ratios of $S_p \approx 55 \pm 5$ sr at 355 nm and $S_p \approx 56 \pm 5$ sr at 532 nm. We conclude from the complete set of data that the typical value is $S_p \approx 60$ sr, but neither a distinct wavelength dependence nor a change of S_p due to aging is evident. The accuracy of our S_p-retrievals is approximately ±5 sr under favorable conditions and approximately ±10 sr when the optical depth is low.

6. Summary and Conclusions

[51] We analyzed optical properties of Saharan dust under long range transport conditions during an exceptionally strong event over southern Germany in May/June 2008: for this purpose we evaluated measurements of our two lidar systems MULIS and POLIS at Munich and Maisach. We derived extinction coefficient profiles at $\lambda = 355$ nm and $\lambda = 532$ nm to characterize the vertical distribution of the aerosols. For the optical characterization of the aerosol type we calculated lidar ratios S_p and particle linear depolarization ratios δ_p at both wavelength. Note that assessments of δ_p at 355 nm are very rare in the literature. These intensive optical parameters, together with the Ångström exponent κ, are excellent tools to characterize dust and to distinguish dust from other aerosol types [*Groß et al.*, 2011c]. The results of this event were related to previous measurements in the frame work of SAMUM-1 and SAMUM-2 that were conducted closer to the source region (Morocco and Cape Verde) [*Freudenthaler et al.*, 2009; *Groß et al.*, 2011a]. Thus, possible changes of intensive properties of dust during transport times of less than one week could be studied.

[52] For the far range regime, we found typical values of the depolarization ratio between $0.30 \leq \delta_p \leq 0.35$, with systematic errors of the individual measurements between ±0.01 and ±0.07. Comparison between the depolarization ratios of the "Munich event" and SAMUM-2 shows an increase at 532 nm with transport time. Because of the comparably large systematic errors, a correspondingly strict conclusion for the shorter wavelength is not possible. The errors of δ_p at 532 nm during the dust event over Munich were in fact very small, but again the larger errors at 355 nm prevents us from quantifying the presumably weak wavelength dependence of δ_p. Only in cases when the systematic errors of the retrieval were small at both wavelengths (during SAMUM-2), the wavelength dependence of δ_p (i.e. an increase of δ_p with λ) could be determined. Thus, we cannot decide yet whether or not the

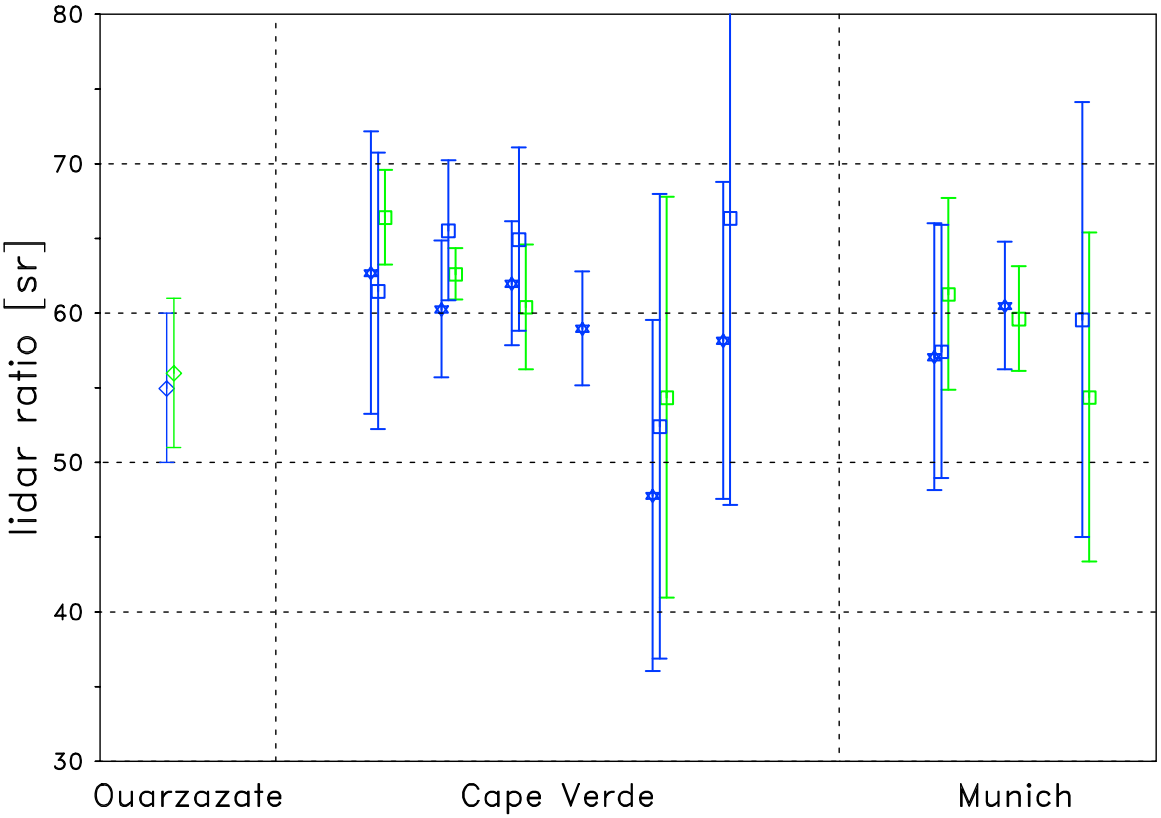

Figure 13. Lidar ratio S_p of Saharan dust at 355 nm (blue; POLIS: stars, MULIS: squares) and 532 nm (green; MULIS: squares) as derived on 6 days in the framework of SAMUM-2 (Cape Verde, 2008) [*Groß et al.*, 2011a] and the 3 days of this study (Munich, 2008). Error bars denote the systematic errors. Lidar ratios from Ouarzazate are mean values derived by *Tesche et al.* [2009].

wavelength dependence of δ_p changes in the long range regime. The outcome of numerical model simulations considering the non-spherical shape of the dust particles [*Gasteiger et al.*, 2011] suggests in general an increase of δ_p with wavelength, but demonstrates as well that this wavelength dependence is very sensitive to the microphysical properties of the particles. As a consequence, for a deeper understanding of the optical properties of dust, high precision lidar measurements of $\delta_p(\lambda)$ are indispensable, preferably in conjunction with additional, independent measurements that can be used for validation and consistency checks of simulations. The benefit of δ_p at longer wavelengths, e.g. at 1064 nm, should be discussed.

[53] Typical values of the lidar ratio of the dust over Munich were $S_p \approx 59$ sr, with errors between ±4 sr and more than ±10 sr for individual cases. These S_p-values are very close to the values from the SAMUM campaigns, i.e., $S_p \approx 60$ sr. No wavelength dependence of S_p could be resolved during the dust event, which is consistent with the previous measurements.

[54] Though the dust event of May 2008 was a very good test bed to investigate intensive properties of transported dust, it would be highly desirable to have more measurements in the far-range regime. In Munich, "severe dust events" occur in the order of one every one or two years, so the number of cases will remain quite small. A candidate for further studies could be a site in the Caribbean Sea, e.g. Barbados, which is located in the main pathway of the outflow of Saharan dust [*Prospero and Carlson*, 1981]. With an increasing number of measurements of (Saharan) dust far away from its source, one can also address the question whether optical properties are primarily influenced by the transport path or by the transport time. Ultimately, when a very large number of (quality assured lidar) measurements will be available, the influence of different source regions of the Saharan desert on the optical properties of dust and their temporal changes can be investigated. From these studies the influence of aging and the origin of the dust might be separated, however, they will be quite expensive as they must include airborne in-situ observations and detailed transport model calculations. The outcome could have significant consequences on potential parameterizations of dust parameters for remote sensing applications and numerical weather prediction.

[55] **Acknowledgments.** We gratefully acknowledge the financial support for the improvement of the EARLINET infrastructure by the European Commission under grant RICA-025991. The authors gratefully acknowledge the NOAA Air Resources Laboratory (ARL) for the provision of the HYSPLIT transport and dispersion model and the READY Web site (http://www.arl.noaa.gov/ready.php) and the Bayerisches Landesamt für Umwelt (LfU), Augsburg, Germany, for the PM10 data of Andechs.

References

Ansmann, A., U. Wandinger, M. Riebesell, C. Weitkamp, and W. Michaelis (1992), Independent measurement of extinction and backscatter profiles in cirrus clouds by using a combined Raman elastic-backscatter lidar, *Appl. Opt.*, *31*, 7113–7131.

Ansmann, A., et al. (2003), Long-range transport of Saharan dust to northern Europe: The 11–16 October 2001 outbreak observed with EARLINET, *J. Geophys. Res.*, *108*(D24), 4783, doi:10.1029/2003JD003757.

Bösenberg, J., et al. (2003), EARLINET: A European Aerosol Research Lidar Network to Establish an Aerosol Climatology, *MPI Rep. 348*, 192 pp., Max-Planck-Inst. für Meteorol., Hamburg, Germany.

Bruckmann, P., W. Birmili, W. Straub, M. Pitz, D. Gladtke, U. Pfeffer, H. Hebbinghaus, S. Wurzler, and A. Olschewski (2008), An outbreak of Saharan dust causing high PM10 levels north of the Alps, *Gefahrst. Reinh. Luft*, *68*(11/12), 490–498.

Cakmur, R. V., R. L. Miller, J. Perlwitz, I. V. Geogdzhayev, P. Ginoux, D. Koch, K. E. Kohfeld, I. Tegen, and C. S. Zender (2006), Constraining the magnitude of the global dust cycle by minimizing the difference between a model and observations, *J. Geophys. Res.*, *111*, D06207, doi:10.1029/2005JD005791.

Córdoba-Jabonero, C., et al. (2011), Synergetic monitoring of Saharan dust plumes and potential impact on surface: A case study of dust transport from Canary Islands to Iberian Peninsula, *Atmos. Chem. Phys.*, *11*, 3067–3091.

Delany, A. C., A. C. Delany, D. W. Parkin, J. J. Griffin, E. D. Goldberg, and B. E. F. Reimann (1967), Airborne dust collected at Barbados, *Geochim. Cosmochim. Acta*, *31*(5), 885–909, doi:10.1016/S0016-7037(67)80037-1.

Draxler, R. R. (1988), Hybrid Single-Particle Lagrangian Integrated Trajectories (HY-SPLIT): Model description, *NOAA Tech. Memo. ERL ARL-166*, 34 pp., Air Resour. Lab, Silver Spring, Md. [Available at http://www.arl.noaa.gov/HYSPLIT_info.php.]

Fernald, F. G. (1982), Analysis of atmospheric lidar observations: Some comments, *Appl. Opt.*, *23*, 652–653.

Freudenthaler, V., et al. (2009), Depolarization-ratio profiling at several wavelengths in pure Saharan dust during SAMUM 2006, *Tellus, Ser. B*, *61*, 165–179.

Gasteiger, J., M. Wiegner, S. Groß, V. Freudenthaler, C. Toledano, M. Tesche, and K. Kandler (2011), Modeling lidar-relevant optical properties of complex mineral dust aerosols, *Tellus, Ser. B*, *63*, 725–741. doi:10.1111/j.1600-0889.2011.00559.x.

Gimmestad, G. G. (2008), Reexamination of depolarization in lidar measurements, *Appl. Opt.*, *47*(21), 3795–3802.

Groß, S., V. Freudenthaler, C. Toledano, and M. Wiegner (2008), Mini-Lidar measurements of particle depolarization and Raman-scattering of Saharan dust and biomass burning at 355 nm during SAMUM2, paper presented at 24th International Laser Radar Conference, Univ. of Colo. at Boulder, Boulder.

Groß, S., M. Wiegner, V. Freudenthaler, and C. Toledano (2011a), Lidar ratio of Saharan dust over Cape Verde Islands: Assessment and error calculation, *J. Geophys. Res.*, *116*, D15203, doi:10.1029/2010JD015435.

Groß, S., M. Tesche, V. Freudenthaler, C. Toledano, M. Wiegner, A. Ansmann, D. Althausen, and M. Seefeldner (2011b), Characterization of Saharan dust, marine aerosols and mixtures of biomass burning aerosols and dust by means of multi-wavelength depolarization and Raman measurements during SAMUM 2, *Tellus, Ser. B*, *63*, 706–724. doi: 10.1111/j.1600-0889.2011.00556.x.

Groß, S., V. Freudenthaler, M. Wiegner, J. Gasteiger, A. Geiß, and F. Schnell (2011c), Dual-wavelength linear depolarization ratio of volcanic aerosols: lidar measurements of the Eyjafjallajökull plume over Maisach, Germany, *Atmos. Environ.*, doi:10.1016/j.atmosenv.2011.06.017, in press.

Guerrero-Rascado, J. L., F. J. Olmo, I. Avilés-Rodríguez, F. Navas-Guzmán, D. Pérez-Ramírez, H. Lyamani, and L. Alados-Arboledas (2009), Extreme Saharan dust event over the Southern Iberian Peninsula in September 2007: Active and passive remote sensing from surface and satellite, *Atmos. Chem. Phys.*, *9*, 8453–8469.

Heintzenberg, J. (2009), The SAMUM-1 experiment over southern Morocco: Overview and introduction, *Tellus, Ser. B*, *61*, 2–11.

Holben, B. N., et al. (1998), AERONET—A federated instrument network and data archive for aerosol characterization, *Remote Sens. Environ.*, *66*, 1–16.

Klett, J. D. (1985), Lidar inversion with variable backscatter/extinction ratios, *Appl. Opt.*, *24*, 1638–1643.

Mattis, I., A. Ansmann, D. Mueller, U. Wandinger, and D. Althausen (2002), Dual-wavelength Raman lidar observations of the extinction-to-backscatter ratio of Saharan dust, *Geophys. Res. Lett.*, *29*(9), 1306, doi:10.1029/2002GL014721.

Mona, L., A. Amodeo, M. Pandolfi, and G. Pappalardo (2006), Saharan dust intrusions in the Mediterranean area: Three years of Raman lidar measurements, *J. Geophys. Res.*, *111*, D16203, doi:10.1029/2005JD006569.

Morris, V., P. Clemente-Colón, N. R. Nalli, E. Joseph, R. A. Armstrong, Y. Detrés, M. D. Goldberg, P. J. Minnett, and R. Lumpkin (2006), Measuring trans-Atlantic aerosol transport from Africa, *Eos Trans. AGU*, *87*(50), 565, doi:10.1029/2006EO500001.

Myhre, G., et al. (2005), Intercomparison of satellite retrieved aerosol optical depth over ocean during the period September 1997 to December 2000, *Atmos. Chem. Phys.*, *5*, 1697–1719.

Nickovic, S., G. Kallos, A. Papadopoulos, and O. Kakaliagou (2001), A model for prediction of desert dust cycle in the atmosphere, *J. Geophys. Res.*, *106*(D16), 18,113–18,129.

Papayannis, A., et al. (2008), Systematic lidar observations of Saharan dust over Europe in the frame of EARLINET (2000–2002), *J. Geophys. Res.*, *113*, D10204, doi:10.1029/2007JD009028.

Penner, J. E., et al. (2001), Aerosols, their direct and indirect effects, in *Climate Change* 2001*: The Scientific Basis. Contribution of Working Group I to the Third Assessment Report of the Intergovernmental Panel on Climate Change*, edited by J. T. Houghton et al., chap. 5, pp. 291–336, Cambridge Univ. Press, Cambridge, U. K.

Prospero, J. M., and T. N. Carlson (1972), Vertical and areal distribution of Saharan dust over the western equatorial North Atlantic Ocean, *J. Geophys. Res.*, *77*, 5255–5265, doi:10.1029/JC077i027p05255.

Prospero, J. M., and T. N. Carlson (1981), Saharan air outbreaks over the tropical North Atlantic, *Pure Appl. Geophys.*, *119*, 677–691, doi:10.1007/BF00878167.

Sokolik, I. N., D. M. Winker, G. Bergametti, D. A. Gillette, G. Carmichael, Y. J. Kaufman, L. Gomes, L. Schuetz, and J. E. Penner (2001), Introduction to special section: Outstanding problems in quantifying the radiative impacts of mineral dust, *J. Geophys. Res.*, *106*(D16), 18,015–18,027, doi:10.1029/2000JD900498.

Tegen, I., A. A. Lacis, and I. Fung (1996), The influence on climate forcing of mineral aerosol from disturbed soils, *Nature*, *308*, 419–422.

Tesche, M., et al. (2009), Vertical profiling of Saharan dust with Raman lidars and airborne HSRL in southern Morocco during SAMUM, *Tellus, Ser B*, *61*, 144–164.

Wiegner, M., W. Kumpf, V. Freudenthaler, I. Stachlewska, and B. Heese (2002), Surface aerosol layer: Annual cycle and parameterization, in *Lidar Remote Sensing in Atmospheric and Earth Sciences*, edited by L. Bissonnette, G. Roy, and G. Vallée, pp. 321–324, U.S. Dep. of Energy, Quebec, Que., Canada.

Wiegner, M., J. Gasteiger, S. Groß, F. Schnell, V. Freudenthaler, and R. Forkel (2011), Characterization of the Eyjafjallajökull ash-plume: Potential of lidar remote sensing, *J. Phys. Chem. Earth*, doi:10.1016/j.pce.2011.01.006, in press.

Winker, D. M., W. H. Hunt, and M. J. McGill (2007), Initial performance assessment of CALIOP, *Geophys. Res. Lett.*, *34*, L19803, doi:10.1029/2007GL030135.

Zender, C. S., R. L. Miller, and I. Tegen (2004), Quantifying mineral dust mass budgets: Terminology, constraints, and current estimates, *Eos Trans. AGU*, *85*, 509, doi:10.1029/2004EO480002.

V. Freudenthaler, J. Gasteiger, S. Groß, F. Schnell, and M. Wiegner, Meteorological Institute, Ludwig-Maximilians-Universität, Theresienstraße 37, D-80333 München, Germany. (volker.freudenthaler@lmu.de; josef.gasteiger@lmu.de; silke.gross@dlr.de; franziska.schnell@physik.uni-muenchen.de; m.wiegner@lmu.de)